Kaposi Sarcoma Herpesvirus (KSHV) vFLIP Induces B-cell Transdifferentiation and Tumorigenesis in Mice

Gianna Ballon, Kang Chen, Rocio Perez, Wayne Tam, and Ethel Cesarman

Supplemental data

1) Supplemental figures and legends

Supplemental Figure 1, related to Figure 1;

Supplemental Figure 2, related to Figure 2;

Supplemental Figure 3, related to Figure 3;

Supplemental Figure 4, related to Figure 3;

Supplemental Figure 5, related to Figure 4;

Supplemental Figure 6, related to Figure 6;

Supplemental Figure 7, related to Figure 6;

Supplemental Figure 8

2) Supplemental methods;

3) Supplemental references.

Supplemental figures and legends

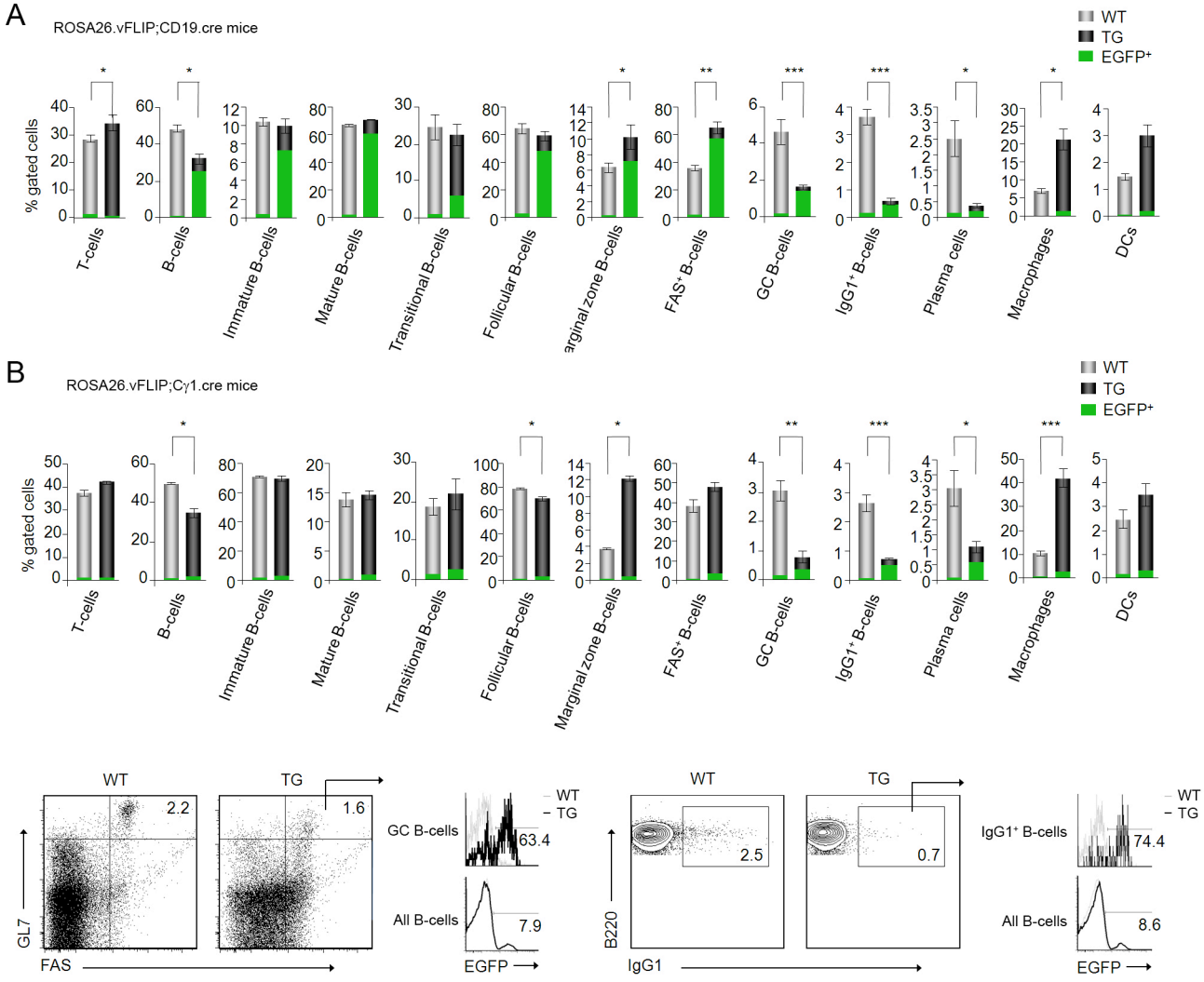

Supplemental Figure 1, related to Figure 1. Effect of vFLIP expression on B-cell differentiation. (A) Flow cytometry analysis performed on splenocytes derived from ROSA26.vFLIP;CD19.cre mice. T cells and various B-cell subsets were evaluated, including total B-cells, immature ($B220^+IgD^-IgM^+$), mature ($B220^+IgD^+IgM^-$), follicular ($B220^+CD21^-CD23^+$), marginal zone ($B220^+CD21^+CD23^-$), transitional ($B220^+CD21^-CD23^-$), FAS^+, GC ($B220^+GL7^+FAS^+$), IgG1-expressing B-cells and plasma cells ($B220^-CD138^+$). Splenic macrophages ($SSC/FSC^{hi}B220^-Gr1^+$) and DCs ($SSC/FSC^{hi}B220^-CD11c^+$) were also evaluated. The percentage of $EGFP^+$ cells within each population is reported (green). (B) The above listed cell populations were also analyzed in ROSA26.vFLIP;Cγ1.cre mice. EGFP expression is

specifically turned on at the GC stage upon activation of the Cγ1 promoter, as assessed by comparing EGFP levels in all B-cells with those in either GC or $IgG1^+$ B-cells (lower panel). *P<0.05, **P<0.005 and ***P<0.005 (two-tailed unpaired Student's t-test). Data represent one of three experiments with similar results (error bars, SEM); at least three TG and control animals were analyzed in each experiment.

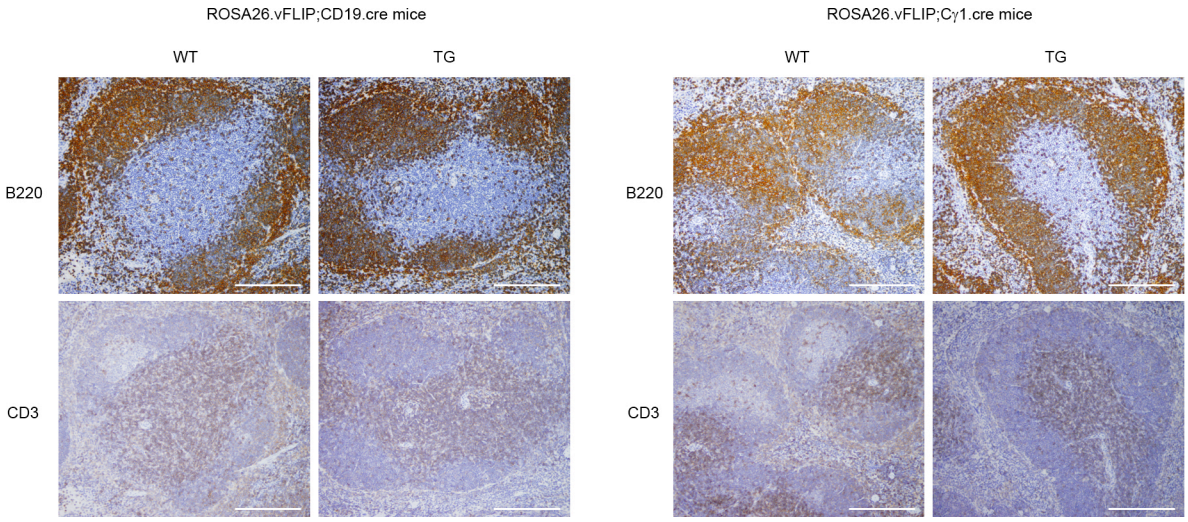

Supplemental Figure 2, related to Figure 2. Preserved B- *versus* T-zone architecture in B-cell specific vFLIP TG mice. B220 and CD3 immunostaining of B- and T-zone, respectively, in both ROSA26.vFLIP;CD19.cre (left panel) and ROSA26.vFLIP;Cγ1.cre mice (right panel). Scale bar, 200 μm.

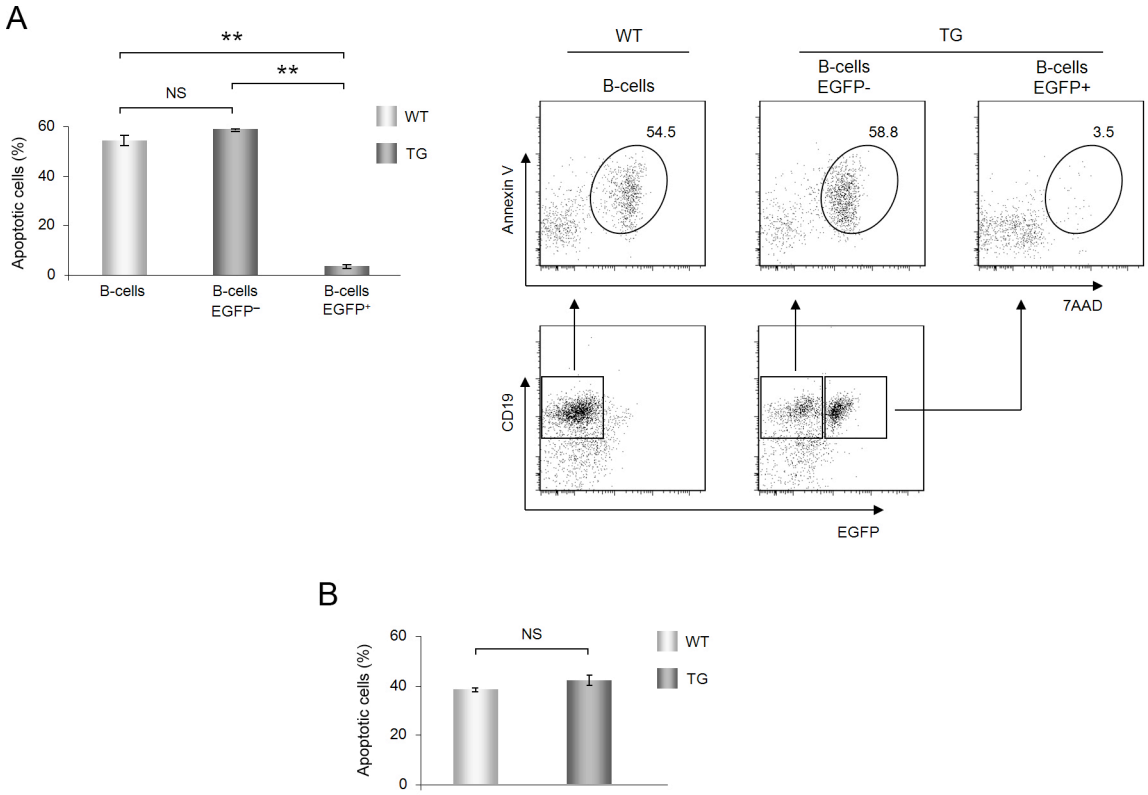

Supplemental Figure 3, related to Figure 3. Impairment of FAS-mediated apoptosis in vFLIP TG B-cells. Splenocytes isolated from either WT or TG ROSA26.vFLIP;CD19.cre mice were treated with 15 µg/ml anti-FAS (Jo2) for 24 hrs, and apoptosis was assessed by Annexin V and 7AAD staining in either WT, TG EGFP^{-} or TG EGFP^{+} CD19^{+} B-cells (A) as well as in T-cells (B). ***P*<0.005 (two-tailed unpaired Student's t-test). Data represent two experiments in which three TG and control animals were analyzed (error bars, SEM).

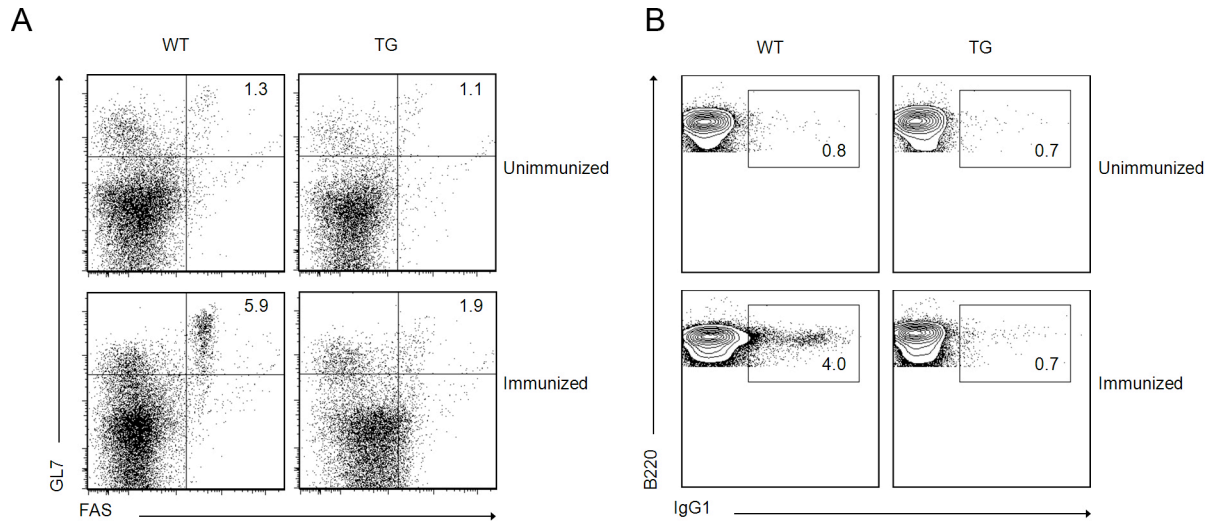

Supplemental Figure 4, related to Figure 3. Impairment of GC formation and IgG1 production in ROSA26.vFLIP;CD19.cre. Flow cytometry showing that GC (A) and IgG1^{+} B-cells (B) failed to develop upon immunization with SRBC (lower panel) and remain at similar levels as in unimmunized mice (upper panel).

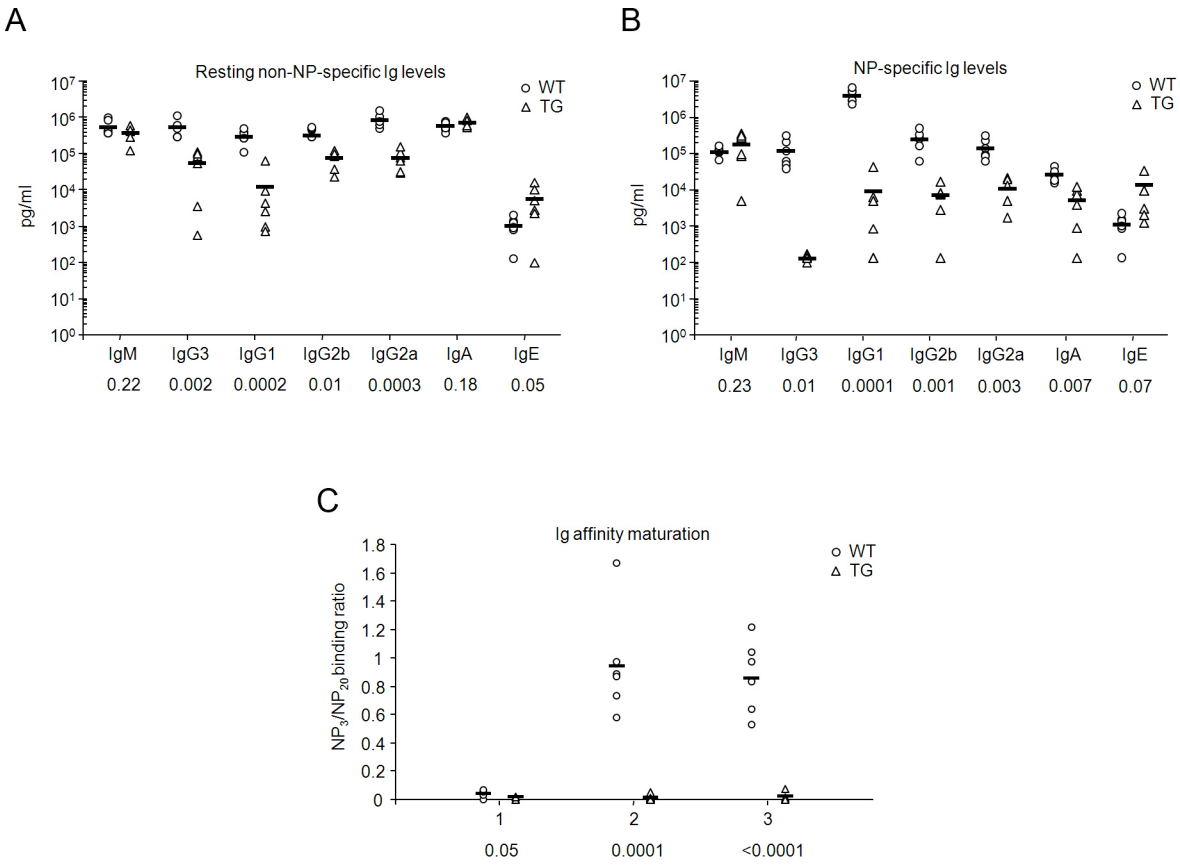

Supplemental Figure 5, related to Figure 4. Serum antibody concentration and Ig affinity maturation in ROSA26.vFLIP;Cγ1.cre mice. Antibody levels were analyzed by ELISA. *P*-values derived from Student's t-test on the means (bars) of WT *versus* TG mice are given below each subclass in the graphs. (A) Resting serum antibody levels evaluated on pre-immune serum samples. (B) NP-specific antibody responses referred to the second boost. (C) Lack of affinity maturation. Higher NP_3/NP_{20} binding ratios indicate the presence of higher-avidity (i.e., affinity-matured) IgG1 antibodies. Post-switched transcripts were barely detectable (data not shown).

A

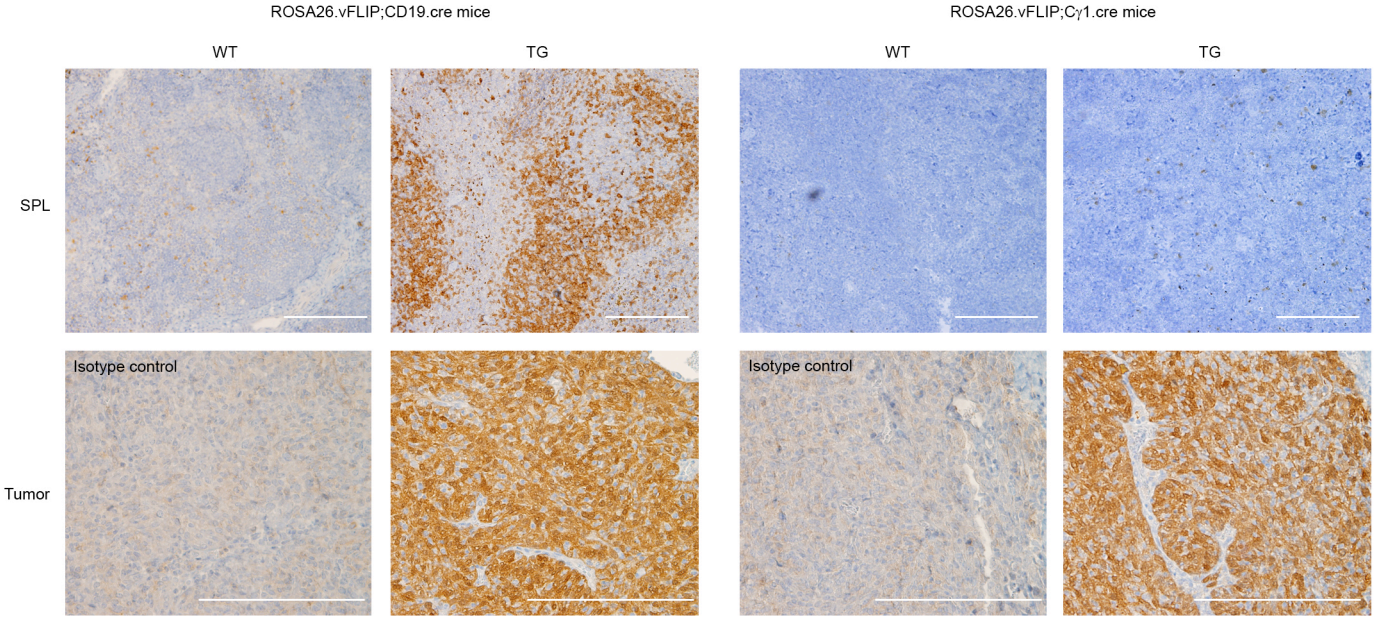

B

```
                    <---------- FR1-IMGT ---------->_____________ CDR1-IMGT __________<-------------------- FR2-IMGT ------------------->__________ CDR2-IMGT ____
seq                 .....gaagatccctgactctcctgtgcagcctcaggattcgatttt...........agtagatactggatgagttgggtccggcaggctccagggaaagggctagaatggattggagaaattaatccagat......agcagtacg
AJ851868 IGHV4-1*02 ctgga-g-tcc-tgaa-------------------------------...........-------------------------------------------------------------------------------------.....---------
AC073563 IGHV4-2*01(P) ctgga-g-tcc-tgaa-------------------------------...........----a-g-----------------------a-----------------a-----------------g-.....---------
AC079273 IGHV4-1*01 ctgga-g-tcc-tgaa-----------------------a--------...........-----------------------t----g--------------a-------------------------------.....--------a
AJ851868 IGHV4-2*02 ctgga-g-tcc-tgaat------------------------------...........-----------------------ct----------------------ag-------------------------ga.....---------
AJ851868 IGHV11-2*02 ctggg-ggtca-ggg-------t----a--g------g--tac----...........---g-c-t---------c-----t--a---a-a--t-----gacc--g--g-----------c------t-t---.....g-----g-a

                    ___<------------------------------------------------------ FR3-IMGT ------------------------------------------------------>________ CDR3-IMGT _______
seq                 ataaactatacgccatctctaaag...gataaattcatcatctccagagacaacgccaaaaatacgctgtacctgcaaatgagcaaagtgagatctgaggacacagccctttattactgtgcatctacggactggtacttcgatgtc
AJ851868 IGHV4-1*02 ------------------------...-------------------------------------------------------------------------------------------------agac-
AC073563 IGHV4-2*01(P) ----------t------------...-------------------------------------------------------------------------------------------------agac-
AC079273 IGHV4-1*01 ---------g-a------------...-------------------------------------------------------------------------------------------------aga
AJ851868 IGHV4-2*02 ------------------------...-------------------------------------------------------------------------------------------------agact
AJ851868 IGHV11-2*02 --------cg-a-----ca-----...---cg-----ct----t---------t-a---g-gc--c----------g--------t---c----------------acg----t----atgagata
```

Supplemental Figure 6, related to Figure 6. Topographic distribution of EGFP+ cells within spleen and tumor sections and productive Ig rearrangements in these tumors. (a) Immunohistochemistry for EGFP was performed in both spleen (upper panel) and tumor (lower panel) samples from either ROSA26.vFLIP;CD19.cre or ROSA26.vFLIP;Cγ1.cre mice. Scale bar, 200 μm. (b) Productive Ig rearrangment sequence from a representative case is shown. Displayed is the alignment from FR1 to CDR3 obtained by comparing the tumor sequence to the IMGT/V-QUEST database (http://www.imgt.org). FR, framework region; CDR, complementary determining region.

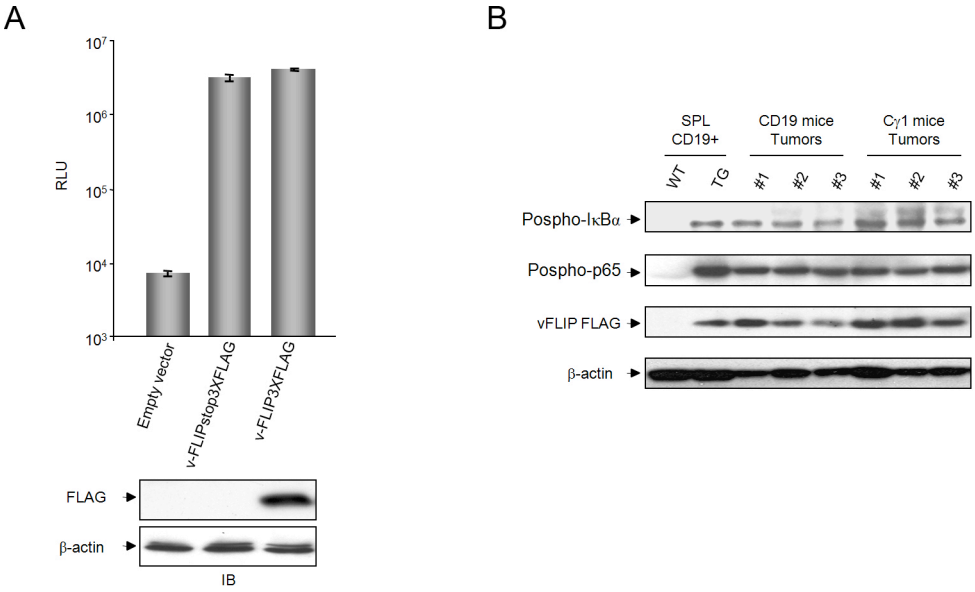

Supplemental Figure 7, related to Figure 6. vFLIP activates NF-κB pathway *in vitro* and *in vivo*. (A) The C-terminal vFLIP-flagged plasmid containing the genetic cassette used to target ROSA26 locus was *in vitro* transiently co-transfected into 293-T cells along with an NF-κB firefly luciferase reporter plasmid. Luciferase assays results are reported as relative luciferase units (RLU) normalized to renilla luciferase. (B) Activation of NF-κB pathway by vFLIP was further confirmed *in vivo* by assessing Pospho-IkBα and Pospho-p65 in WT and TG $CD19^{+}$ B-cells isolated from ROSA26.vFLIP;CD19.cre mice as well as in tumor samples.

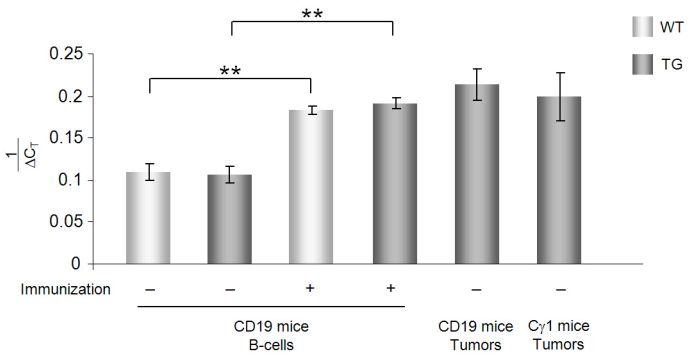

Supplemental Figure 8. miR155 expression levels in B-cells and tumors samples. miR155 was quantified by quantitative real-time RT-PCR in B-cells derived from ROSA26.vFLIP;CD19.cre and tumors derived from both vFLIP TG lines. **P*<0.05 (two-tailed unpaired Student's t-test). A representative experiment is shown in which 4 samples per category were analyzed (error bars, SEM).

Supplemental methods

Flow Cytometry

The following fluorescent-labeled anti-mouse antibodies were used: APC- or PerCP-conjugated anti-B220 (RA3-6B2), R-PE-conjugated anti-CD23 (B3B4), APC-conjugated anti-CD21/CD35 (7G6), R-PE-conjugated anti-CD38 (90), R-PE-conjugated anti-CD27 (LG.3A10), APC-conjugated anti-CD138 (281-2), R-PE-conjugated anti-CD90.2 (53-2.1), APC-conjugated anti-IgM (II/41), PE-conjugated anti-IgD (11-26c.2a), PE-conjugated anti-IgG1 (A85-1), PE-conjugated anti-CD95 (Jo2), PerCP-Cy5.5-conjugated anti-CD19 (1D3), PE-conjugated anti-Gr1 (RB6-8C5) and APC-conjugated Annexin V. All antibodies were from BD Pharmingen, except for Alexa Fluor700-conjugated anti-CD19 (6D5; Biolegend), biotin-conjugated anti-λ (SouthernBiotech), R-PE-conjugated anti-κ (SouthernBiotech), PNA (Vector Laboratories), biotinylated anti-GL7 (GL7; eBioscience) and anti-CD11c (N418; Miltenyi). Biotinylated PNA and biotinylated anti-λ and anti-GL7 were developed with either streptavidin-PerCP (BD Pharmingen) or Streptavidin-Pacific Orange (Invitrogen Molecular Probe) protein conjugates.

RT-PCR

Total RNA was isolated from thymus as well as $CD19^+$ and $CD19^-$ splenocytes using TRIZOL reagent (Invitrogen). DNase-treated total RNA was reverse transcribed into cDNA using Reverse Transcription System and oligodT primers (Promega), following manufacturer's instructions, and used for RT-PCR. Two μl of cDNA were added to a PCR reaction containing 10 pmol of each primer, 200 mM dNTP, 10 mM Tris- HCl (pH 8.3), 50 mM KCl, and 4.5 mM $MgCl_2$ in a final reaction volume of 25 μl. Initial denaturation was performed at 95°C for 2 min, followed by 34 cycles at 95°C for 15 sec, 56°C for 15 sec, and 72°C for 1 min, followed by a final primer extension at 72°C for 7 min. The following primer sets were used: vFLIP3XFLAG (5'-

TTCCACACAGATTCGCACAGA-3'; 5'-GGCACGCCACCAGACAA-3'), CRE (5'-CGTCGGTAGCGGCTTCA-3'; 5'-GGCTATGCCAGCGTCGAGTA-3') EGFP (5'-GGTGATGTTCTGAGTACATAGCGG-3'; 5'-CCGAGGACGAAATGGAAGTG-3'); β-actin (5'-GGAGTCAACGGATTTGGTCGTA-3', 5'- GGCAACAATATCCACTTTACCAGAGT-3'). Primers to detect the Ig germline and post-switch transcripts have been previously described (1).

Transient transfection and luciferase assay

vFLIP-encoding plasmid was co-transfected into 293-T cells with an NF-κB firefly luciferase reporter plasmid carrying an Ig promoter as previously reported (22). Three independent experiments were performed. The transfections were carried out in triplicates and in the presence of pRSV-RL (Promega), a renilla luciferase-encoding plasmid, to normalize the results for the transfection efficiency. Cells were harvested 48 hrs post transfection and cell lysates were prepared as specified by the manufacturer (Promega). Luciferase assay absorbances were measured on a luminometer (Dynex Tech).

Quantitative real-time RT-PCR

Quantitative real-time RT-PCR was performed on ABI Prism 7000 Sequence Detection System (Applied Biosystems) with miR155 Taqman MicroRNA Assay kit (Applied Biosystems), following the manufacturer's instructions. All reactions were done in triplicates and C_T values were calculated. For normalization purposes, ΔC_T values were obtained by subtracting miRU6 C_T values from those of miR155 and results are shown as $1/\Delta C_T$. A representative experiment is shown in which 4 samples per category were analyzed (error bars, SEM).

Supplemental references

1. Muramatsu, M., Kinoshita, K., Fagarasan, S., Yamada, S., Shinkai, Y., and Honjo, T. 2000. Class switch recombination and hypermutation require activation-induced cytidine deaminase (AID), a potential RNA editing enzyme. *Cell* 102:553-563.